Deposition of tin containing carbon amorphous composite films by thermionic vacuum arc technique

V. IONESCU[*], C. P. LUNGU[a], M. OSIAC[b]
Department of Physics, Ovidius University, Constanta, 900527, Romania
[a]National Institute for Laser, Plasma and Radiation Physics, Magurele, 077125, Romania
[b]Faculty of Physics, University of Craiova, Craiova, 200585, Romania

The paper presents the synthesis of Sn-containing carbon amorphous composite films deposited by the thermionic vacuum arc technique. The chemical composition, morphology, microstructure and crystallographic properties of the films were investigated by energy-dispersive spectroscopy (EDS), scanning electron microscopy (SEM), low-angle X-ray diffraction (XRD) and X-ray photoelectron spectroscopy (XPS). The friction coefficients of the prepared films analyzed by a CSM ball-on-disk tribometer sliding against sapphire balls in dry conditions at room temperature were found to be 0.12 to 0.14, which is two to four times lower than that of the substrate material.

1. Introduction

The metal–containing amorphous carbon (a-C:Me) or tetrahedral (diamond-like) amorphous carbon (ta-C:Me) films have attracted much research interest in a wide range of engineering applications: implantable medical devices [1], RF MEMS switches [2], and solid lubricant coatings [3] due to their excellent tribological properties such as low hardness, high wear resistance and low friction.

It was reported that the hydrogen-free a-C coatings deposited by various methods (pulsed laser deposition, filtered cathode vacuum arc) [4,5] have high residual stress acquired during the deposition process, which limits the coating thickness to less than 2 μm since residual stress weakens the adhesion strength of coatings on substrates[6]. A coating thickness of less than 2 μm is not suitable for severe tribological applications where long working life is crucial. Pure a-C also exhibits brittle behavior at applied high load [7], thus its load-bearing capability is limited.

The incorporation of metals into hydrogen free a-C matrix is an effective way in the reduction of residual stress. However, hardness of the coating suffers: about 60% of the coating hardness was lost when it was doped with only 10 at.% of aluminium [8]. One way to bring back the coating hardness is by strain release via nanosized metal-based crystallites sliding in the amorphous carbon matrix.

The aim of this paper is to study Sn-containing amorphous carbon composite films deposited by the thermionic vacuum arc (TVA) method from the point of view of elemental composition, atomic bonds formed at the surface and bulk, and to correlate the wear resistance features with the mechanical properties (coefficient of friction) by variation of the Sn atomic percentage in the films.

2. Experimental

The method used here based on the TVA technique for deposition of the Sn-containing carbon amorphous composite films was described in detail elsewhere [9,10]. It uses two identical TVA gun set-ups that produce two separate electron beams emitted by externally heated cathodes. Each cathode is made from a tungsten wire with a diameter of 1 millimetre. The electron beams are accelerated by high anodic voltages and simultaneously bombard the graphite rod of 10 millimetre diameter and 150 millimetre length and the TiB_2 crucible containing 99.99 percent purity Sn metal, as shown in Fig.1.

Applying a high voltage between 1 and 6 kV on each of the anode-cathode sets, two independent plasmas were formed in the pure carbon and Sn vapours. Due to the high energy dissipated in the unit plasma volume, the material was strongly dispersed and completely droplet-free. The chamber was pumped with mechanical and diffusion pumps until a pressure of 5×10^{-5} Pa was obtained.

The currents used to heat the cathode filaments were 42 A for carbon and 55 A for Sn, respectively. The current of the discharge running in the C vapours was $I_{disch} = 1$ to 1.4 A at a voltage of $U_{disch} = 1400$ -1700 V. In the case of the discharge running in the Sn vapours, the current intensity was $I_{disch} = 0.45$ - 0.95 A and $U_{disch} = 900$ - 1100 V, respectively. The deposition rate r_d and the film thickness d were measured and controlled in situ using a FTM7 quartz microbalance.

The first layer deposited was Sn with a thickness of 300 nm, followed by the C-Sn composite layer, having a

total thickness of 2 μm. The deposition rate for the C-Sn layer was 0.26 to 0.37 nm/s.

The substrates were AISI 316L stainless steel polished disks, with 25 millimeters in diameter and 3 millimeters in thickness, and BK7 optical glass disks with the same diameter and 1 millimeter in thickness.

The investigated film samples were located at the P_1 position, closest to the C crucible, the P_2 position located on the mid-distance between anodes and the P_3 position closest to the Sn crucible, as seen in Fig. 1. The substrates were kept at 200°C during depositions. The distance between the C crucible and the P_1 sample was 350 millimeters, equal to the distance between the Sn crucible and the P_3 sample, and the distance between the C crucible and the P_2 sample was 400 millimeters.
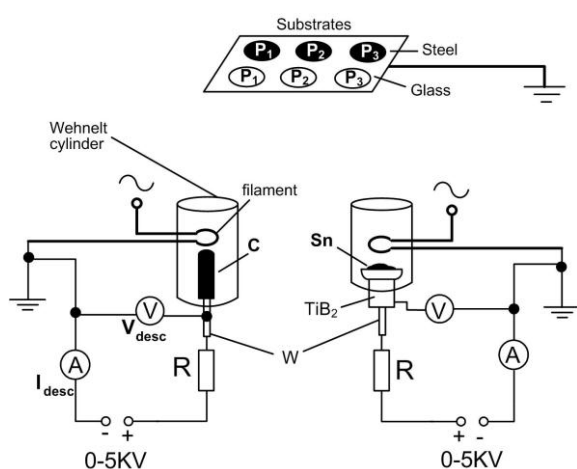
Fig. 1. The experimental set-up for the C-Sn composite film deposition.

The first layer deposited on substrates was a Al layer (with the thickness of 300 nm), followed by the C-Al composite layer, having a thickness of 2 μm. The friction coefficient measurements were performed using a CSM ball-on-disk tribometer consisting of rotating disks (our samples) sliding on stationary Safire balls (6 mm in diameter) at a sliding speed of 0.1m/s in dry conditions at room temperature (22°C) and relative humidity of air. Normal load of 1 N and sliding radius of 10mm were chosen in this analysis.

The SEM measurements were carried out using a Philips ESEM XL 30 TMP W scanning electron microscope. The compositional analysis of the film was accomplished using an energy dispersive x-ray spectroscopy microanalysis detector (EDS) attached to the SEM.

The XRD patterns were obtained using a Shimadzu model 6000 thin film diffractometer operating with Cu Kα radiation (45 kV, 40 mA).

The XPS measurements were recorded using a VG ESCA III MK2 spectrometer system equipped with a monochromatic Al Kα X-ray source.

The coefficient of friction and wear resistance measurements were performed using a CSM ball-on-disk tribometer consisting of rotating disks (our samples)

sliding on stationary sapphire balls (6 mm in diameter) with a sliding speed of 0.1 m/s in dry conditions at room temperature, and at the normal loads of 1 N, 3 N, 5 N and 7 N.

3. Results and discussion

Low-angle XRD analyses were performed to establish the presence of crystalline phases in the coatings and to calculate the average crystalline size of the particles. In Fig. 2, the diffractions peaks at 30.65°, 32.10°, 44.02° and 44.96° 2θ were assigned to (200), (101), (220) and (211) planes of the Sn tetragonal phase, showing the existence of Sn crystalline phases in the prepared film.

The peak intensities and the full width at half maximum (FWHM) for all orientations were almost the same, indicating uniform grain size and random orientation.
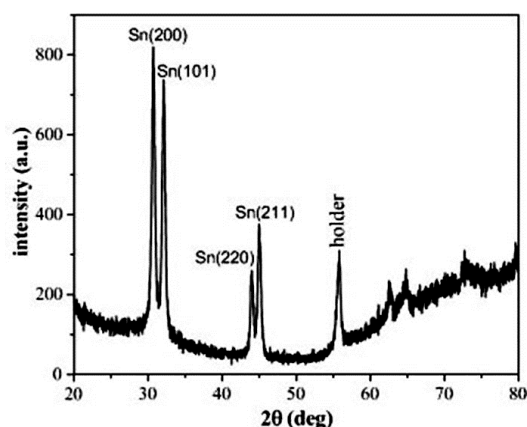
Fig. 2. Typical X-ray diffraction pattern of the C-Sn composite film.

Ignoring the microstraining effect (which affects the XRD peak width), as a first-order approximation, the average crystalline size can be estimated by the Debye – Scherrer formula[11]. The calculated mean grain size of Sn crystallites spreads from 16 to 25 nanometers in the a-C matrix.

D. Manole et al. [12] and V. Ciupina et al. [13] reported from transmission electron microscopy (TEM) measurements realized on the C-Sn composite the formation of Sn particles embedded in the amorphous carbon matrix having dimensions in the range of 10 to 30 nm. Their results are in agreement with Debye-Scherrer's calculation of the mean grain size of the Sn crystallites.

The morphological SEM images of the samples investigated are presented in Fig. 3. In the case of the P_1 sample, the SEM image presented the existence of C-Sn micrometrical conglomerates, separated by areas covered with barely observable formations (under 1 μm) (see Fig. 3a).

The SEM image of the P_2 sample surface presented in Fig. 3b showed the highest number of micrometrical egg-

shaped formations, an appropriate morphology to use the C-Sn composite films as a solid lubricant coating by reducing the contact area between the motion piece and the low friction inner surface of a bearing sleeve assembly.
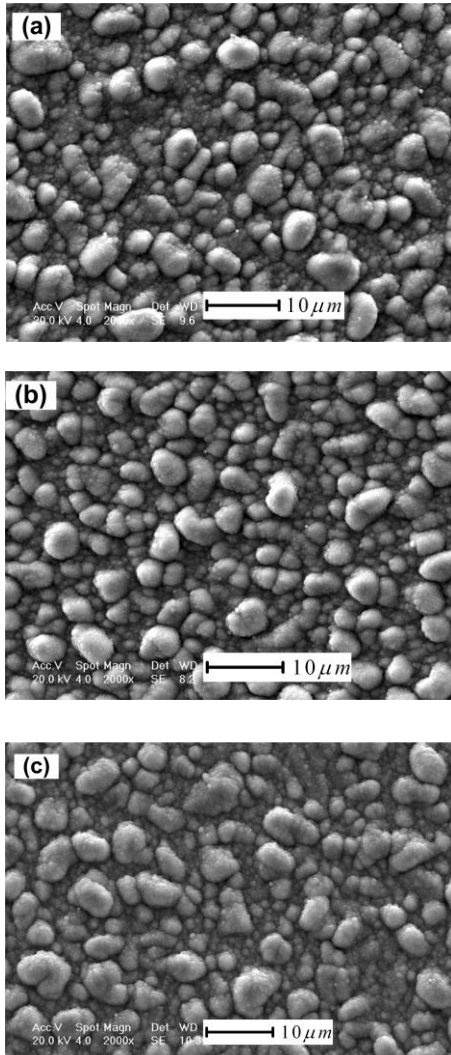
Fig. 3. The morphological SEM images of the C-Sn samples surface: (a) - P_1, (b) - P_2, (c) - P_3.

Fig. 4. SEM images of wear tracks on the C-Sn coatings, after the tribological test: –P_1, (b) – P_2, (c) - P_3.

Table 1. The elemental percentage composition of the deposited C-Sn films resulting from EDS analysis.

C-Sn Samples	C (at. %)	O (at. %)	Sn (at. %)
P_1	58.55	11.73	29.72
P_2	53.50	15.67	30.83
P_3	52.07	14.70	32.42

The SEM images of wear tracks for the P_1, P_2 and P_3 samples are presented in Fig. 4. In the case of the P_2 sample, less intense line scratches and almost no grooves were observed (see Fig. 4b). The appearance of scratch lines and grooves on different C-Sn samples are observed, as seen in Fig. 4a and Fig. 4c, respectively. The morphological investigation showed that the sample P_2, with the most compact structure, has the highest wear resistance.

Using the EDS method, the composition of the three C-Sn films was measured, and the concentration of each element is presented in Table 1.

The relatively high oxygen concentration indicated by the EDS compositional analysis results from the deposition chamber contamination. The oxygen residual gas, present in the reaction chamber at the working pressure of $5*10^{-5}$ Pa, was included in the growing C-Sn film, as revealed by the EDS compositional analysis.

The XPS technique was used to investigate the oxidation states of Sn (Sn 3d spectra), the C bonding states (C 1s spectra) and the atomic percentage of the elements in the surface chemistry of the material analyzed. As seen in Fig.5, by the Gaussian deconvolution of the Sn 3d individual spectral line of the samples, four peaks were found at the binding energies (BE) of 486.7 eV (A peak),

495 eV (B peak), 485.2 eV (C peak) and 493.3 eV (D peak).

From the standard ESCA spectra of the Sn analyzed samples (P_1, P_2, and P_3) and from the line energy information [14], the appearance of the A and B peaks suggests the Sn^{4+} oxidation state, and the position of the C and D peaks implies the Sn^0 oxidation state of the SnO_2 system.

The XPS results suggest that an important amount of oxygen could form SnO_2 on the film surface, this being a stronger argument to cover the Sn surface clusters with a thin layer of a-C. A similar observation was reported by Chen J.S et al.[15] for iron-containing amorphous carbon films. Me'rel et al.[16] explain that in the deconvoluted C1s spectra, the peak at 284.4eV corresponds to the sp^2 bonding of carbon atoms, and the peak at 285.5 eV corresponds to the sp^3 bonding carbon atoms.
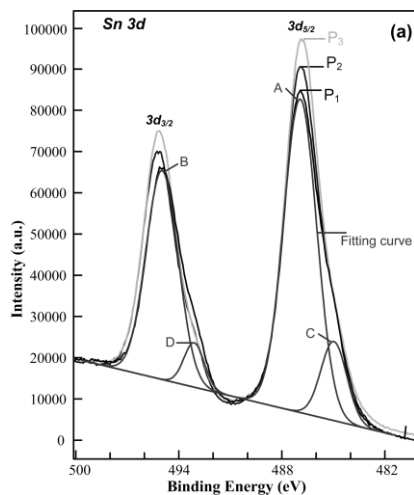
Fig. 5.The Sn3d XPS spectra for the P_1, P_2 and P_3 samples of C-Sn film; the A, B, C and peaks were identified at binding energies of 486.7 eV, 495 eV, 484.7 eV and 493.1 eV, respectively.
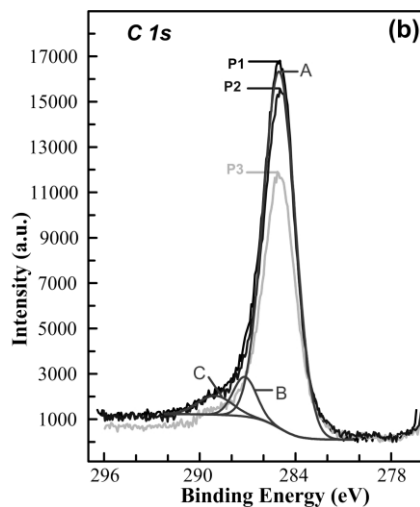
Fig. 6. The C1s XPS spectra for the P_1, P_2 and P_3 samples of C-Sn film; the A, B and C peaks were identified at BE of 285.3 eV, 287.2 eV and 289.2 eV, respectively.

The A peak at BE of 285.4 eV belongs to the C1s spectral line of the P_2 sample shown in Fig. 6, indicating the presence of the C-C bonds. The second and third peaks (B at 287.2 eV and C at 289.1 eV, respectively) may be attributed to C-O and O-C=O contamination formed on the layer surface. From Fig. 5 and Fig. 6, a very minor variation of the C1s and Sn3d (3/2 and 5/2) XPS spectral lines for all C-Sn samples was observed.

The composition of the C-Sn films deposited on stainless steel substrates resulting from XPS quantitative analysis is presented in Table 2, together with the coefficients of friction of the respective coatings.

Table 2. Composition of the C-Sn films resulting from XPS quantitative analysis and coefficient of friction obtained in dry sliding using 6 mm Sapphire balls.

C-Sn Samples	C (at. %)	O (at. %)	Sn (at. %)	μ (1 N load)
P_1	63.3	9.2	27.5	0.24
P_2	58.6	12.5	28.9	0.22
P_3	50.9	11.6	37.5	0.25

A difference in the quantitative evaluation of the relative concentration percentage was observed, due to the different principles of the two analyzing methods (EDS and XPS). While the electron beam penetrates a few micrometers into the material (EDS method), the analyzed volume is very small using the XPS method (the signal is only collected from the sample surface, a few nm in depth) [17]. Y. Inoue et al.[18] reported an increase of the Sn atomic percentage composition after ten seconds of argon ion treatment of a-C:Sn films deposited by RF plasma-enhanced chemical vapor deposition (PECVD).

If the topmost metallic clusters are covered with a layer of a-C, it should be possible to "uncover" them by using Ar^+ ion bombardment with sufficient energy. The explanation of this phenomenon is based on the fact that it accomplished a preferential sputtering, with the a-C layers being removed faster than the Sn clusters. Consequently, the surface has been enriched in Sn.

Fig. 7 shows the coefficient of friction behavior when the applied load varied from 1 to 7 N. The coefficient of friction of the coating (P_2) was at the same value as the stainless steel substrate when the applied load was 1 N. However, when increasing the applied load, the difference between the coefficients of friction of the C-Sn coatings drastically changed in comparison with those of the substrates. The minimum values of 0.12 to 0.14 were found when the applied loads were 3 and 5 N. However, at a 7 N load, the coefficient of friction of the coating slightly increased by approximately 0.25, while the coefficient of friction of the substrate increased by 0.7 to 0.8 up to the seizure. The coating with the best antifriction properties contains 58.6 percent at C, 12.5 percent at O and 28.9 percent at Sn.
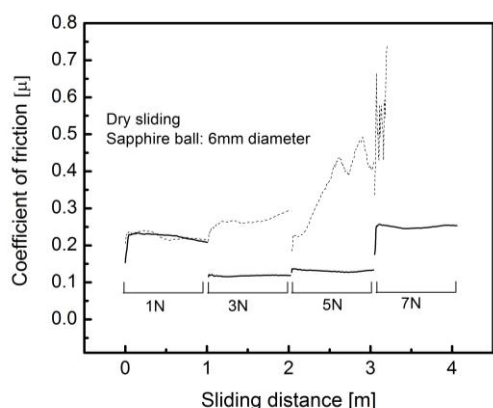
Fig. 7. The variation of the coefficients of friction with sliding distance and load for P₂ sample (solid line) and for stainless steel substrate (dotted line).

The reduced coefficient of friction and increased wear resistance of the P_2 sample may result from the change of shear stress during friction as the C content in the film increased. From the ductility point of view, the Sn inclusion in the prepared layer has an optimum concentration of 30 percent at Sn.

4. Conclusions

The Sn-containing amorphous carbon films with a thickness of 2 μm were successfully deposited onto the stainless steel substrates using the TVA method. The XRD pattern of the prepared films also revealed the presence of Sn crystalline grains, with a mean grain size estimated in the range of 16 to 25 nm. The Sn 3d (3/2 and 5/2) XPS spectra showed the oxidation states of Sn (Sn^0 and Sn^{4+}), and the C1s spectra infer the existence of the sp^3 bonding states of carbon at the film surface. Tribological tests showed that the P_2 sample containing 30 percent Sn concentration in the carbon matrix has the lowest coefficient of friction of 0.12 to 0.14, which is two to four times lower than that of the substrates used in this experiment.

Furthermore, the morphological SEM investigations showed that the P_2 sample has the highest number of micrometrical egg-shaped conglomerates, organized very compactly at the surface. It also presented less intense line scratches, with almost no grooves being marked after the tribological test.

References

[1] P. D. Maguire, T. I. T. Okpalugo, I. Ahmad, Material Science Forum **518**, 477 (2006).
[2] J. C. Orlianges, C. Champeux, A. Catherinot, A. Pothier, P. Blondy, P. Abelard, B. Angleraud, Thin Solid Films **453-454**, 291 (2004).
[3] C. Donnet, A. Erdemir, Tribology Letters **7**, 389 (2004).
[4] Q. Hou, J. Gao, Mod. Phys. Lett. B **11**, 757 (1997).
[5] B. K. Tay, D. Sheeja, Yu L.J., Diamond Relat. Mater. **12**, 185 (2003).
[6] M. Ham, A. Lou, J. Vac. Sci. Technol. A **8**(3), 2143 (1990).
[7] A. Matthew, S. S. Eskildsen, Diamond Relat. Mater. **3,** 902 (1994).
[8] B. K. Tay, Y. H. Cheng, X. Z. Ding, S. P. Lau, X. Shi, G. F. You, D. Sheeja, Diamond Relat. Mater. **10**, 1082 (2001).
[9] C. P. Lungu, I. Mustata, G. Musa , A. M. Lungu, O. Brinza, C. Moldovan, C. Rotaru, R. Iosub, F. Sava, M. Popescu, R. Vladoiu, V. Ciupina, G. Prodan, N. Apetroaei, J. Optoelectron. Adv. Mater. **8**, 74 (2006).
[10] C. P. Lungu, I. Mustata, G. Musa, V. Zaroschi, A. M. Lungu, K. Iwasaki, Vacuum, **76**, 127 (2004).
[11] M. V. Zdujic, O. B. Milosevic, L. Karanovic, Mater. Lett. **13**, 125 (1992).
[12] D. Manole, C. Casapu, O. Pompilian, C. P. Lungu, G. Prodan, V. Ciupina, J. Optoelectron. Adv. Mater. **10**(11), 2954 (2008).
[13] V. Ciupina, R. Vladoiu, A. Mandes, G. Musa, C.P. Lungu, J. Optoelectron. Adv. Mater. **10**(11), 2958 (2008).
[14] C. D. Wagner, W. M. Riggs, L. E. Davis, J. F. Moulder, Handbook of X-ray Photoelectron Spectroscopy, Perkin-Elmer Corporation, USA (1979).
[15] J. S. Chen, S. P. Lau, G. Y. Chen, Z. Sun, Y. J. Li, B. K. Tay, J. W. Chai, Diamond Relat. Mater. **10**, 2018 (2001).
[16] P. Me´rel, M. Tabbal, M. Chaker, S. Moisa, J. Margot, Appl. Surf. Sci. **136**, 105 (1998).
[17] R. V. Ghita, C. Logofatu, C. Negrila, A. S. Manea, M. Cernea, V. Ciupina, M. F. Lazarescu, J. Optoelectron. Adv. Mater. **8**(1), 31 (2006).
[18] Y. Inoue, T. Komoguchi, H. Nakata, O. Takai, Thin Solid Films **322**, 41 (1998).

[*]Corresponding author: ionescu.vio@gmail.com